JPEDAV (2006) 27:5-13
DOI: 10.1361/105497196X92736
1547-7037/$19.00 ©ASM International

Thermodynamic Assessment of the Cu-Pt System

Taichi Abe, Bo Sundman, and Hidehiro Onodera

(Submitted December 20, 2004; in revised form March 3, 2005)

A CALPHAD assessment of the Cu-Pt system has been carried out. Two and four sublattice models were applied to describe the Gibbs free energies of ordered phases where the contribution of SRO is taken explicitly into account through the reciprocal parameters. The disordered fcc A1 and liquid phases were treated as substitutional solutions. A consistent set of parameters for the phases in the Cu-Pt system as obtained, and those parameters can satisfactorily reproduce the experimental phase equilibria and thermodynamic properties, such as enthalpies, activity of Cu, and long-range order parameters.

Keywords compound energy formalism, pair interactions, short range ordering

1. Introduction

Cu-Pt alloys have been investigated intensively over the past few years due to their potential applications as catalysts, an alternative to pure-Pt and Pt-group catalysts.[1,2] Moreover, it has been found that the addition of Cu is effective in decreasing the ordering temperature in the fabrication process of $L1_0$-FePt nanomagnetic materials.[3,4] Consequently, interest has also grown in the Cu-Pt system as one of the subsets of the Cu-Fe-Pt ternary system.

According to the phase diagram reviewed by Subramanian et al.,[5] the Cu-Pt binary system consists of the liquid phase, a continuous solid solution phase, and several ordered phases at low temperatures. At 1:1 stoichiometry, an $L1_1$ ordered phase forms. This intermetallic compound consists of alternative stacking of Cu and Pt layers along the <111> directions and is unique to this binary system. In the Pt-rich region, cubic-$CuPt_3$, rhombohedral-Cu_3Pt_5 and orthorhombic-$CuPt_3$ ordered phases have been proposed by Miida et al.[6] In the Cu-rich region, $L1_2$-Cu_3Pt and one-dimensional long-period structure (LPS) have been observed in compositions around 30 at.% Pt.[7,8] The congruent point for the order-disorder transition of the $L1_2$-Cu_3Pt phase appears around 16 at.% Pt, which is not consistent with its stoichiometric composition. Although several thermodynamic assessments have been done for the liquidus and solidus,[5,9-11] no thermodynamic assessments of the ordered phases at low temperatures have been carried out yet.

In the present assessment, the CALPHAD technique was applied to describe the Gibbs free energy of the liquid, A1(disordered FCC), $L1_2$-Cu_3Pt, and $L1_1$-CuPt stable phases, and $L1_2$-$CuPt_3$ and $L1_0$-CuPt metastable phases in the Cu-Pt system, while other superstructures were ignored due to the lack of thermodynamic and crystallographic information about them. Reciprocal parameters were used to describe the contribution of short-range ordering (SRO) to the Gibbs free energy.

This paper was presented at the International Symposium on User Aspects of Phase Diagrams, Materials Solutions Conference and Exposition, Columbus, Ohio, 18-20 October, 2004.

Taichi Abe, Bo Sundman, and **Hidehiro Onodera,** National Institute for Materials Science, Computational Materials Science Center, 1-2-1 Sengen, Tsukuba, Ibarki 305-0047 Japan. Contact e-mail: Abe.Taichi@nims.go.jp.

2. Experimental Data

Liquidus and solidus temperatures have been measured only in the Cu-rich region.[12,13] At low temperatures, various kinds of ordered structures have been proposed on the basis of experimental measurements. Many studies have been carried out for order-disorder transitions in $L1_2$-Cu_3Pt[14-22] and in $L1_1$-CuPt[14-17,21,23-29] and have been in agreement, while ordered structures in the Pt-rich and peritectoid regions, expected to be in the range of ~30 at.% Pt involving the LPS, have not been established yet.

The enthalpies of mixing in the A1 phase have been measured at 923,[14] 913,[30] and 1350 K,[31,32] Of those mixing enthalpy data, one measured by Weibke et al.[14] was not used in the present assessment because it was significantly different from others. The enthalpies of formation of $L1_2$-Cu_3Pt and $L1_1$-CuPt ordered phases have been measured by Meschel et al.[33] and by Oriani et al.,[30] respectively. For the $L1_2$-$CuPt_3$ and $L1_0$-CuPt metastable phases, the enthalpies of formation have been estimated by theoretical calculations by means of the first-principles method[34-37] and Miedema method.[38]

The activity of Cu has been measured in a wide range of temperatures: 1625,[39] 1573,[13] 1273,[40] 1273 and 1473,[41] and 823-1073 K.[17] The long-range order parameters in $L1_1$-CuPt alloys have been studied by Walker[42] and by Lang et al.[43] The short-range order parameters in the A1 phase have been measured by Saha et al.[44] in alloys with compositions ranging from 7 to 75 at.% Pt at 1173 K, by Walker[42] in CuPt at 1163 K, and by Batirev et al.[45] in a Cu-29 at.% Pt alloy at 773 K and in a Cu-50 at.% Pt alloy at 1173 K.

3. Thermodynamic Models

In the present assessment, the four-sublattice model, two-sublattice model, and substitutional solution model

were applied to describe the Gibbs free energy of the phases in this system. The pure solid elements in their stable states at 298.15 K were chosen as reference states. The Gibbs free energies as a function of temperature for stable and metastable states of the pure elements were taken from the compilation of Dinsdale.[46]

3.1 Solution Phases

The liquid and A1 phases were modeled as a substitutional solution phase. The Gibbs free energy for a solution phase ϕ can be described as:

$$G_m^{\phi} = \sum_{i=\mathrm{Cu}}^{\mathrm{Pt}} x_i \, {}^0G_i^{\phi} + RT \sum_{i=\mathrm{Cu}}^{\mathrm{Pt}} x_i \ln x_i + {}^EG_m^{\phi} \qquad \text{(Eq 1)}$$

where x_i, ${}^0G_i^{\phi}$, R, and T are the mole fractions of an element i, the Gibbs free energy of i with the structure ϕ, the gas constant, and temperature, respectively. The second term on the right-hand side is the ideal entropy term. ${}^EG_m^{\phi}$ is the excess Gibbs free energy term given by:

$${}^EG_m^{\phi} = x_{\mathrm{Cu}} x_{\mathrm{Pt}} L_{\mathrm{Cu,Pt}}^{\phi} \qquad \text{(Eq 2)}$$

The interaction parameter, $L_{\mathrm{Cu,Pt}}^{\phi}$, is composition dependent. In the form of Redlich-Kister polynomials, it can be written as:

$$L_{\mathrm{Cu,Pt}}^{\phi} = \sum_{v=0}^{n} {}^vL_{\mathrm{Cu,Pt}}^{\phi} (x_{\mathrm{Cu}} - x_{\mathrm{Pt}})^v \qquad \text{(Eq 3)}$$

The Redlich-Kister coefficients, ${}^vL_{\mathrm{Cu,Pt}}^{\phi}$, can be temperature dependent as ${}^vL_{\mathrm{Cu,Pt}}^{\phi} = {}^vA^{\phi} + {}^vB^{\phi}T + \cdots$, where ${}^vA^{\phi}$ and ${}^vB^{\phi}$ are fitted to experimental data.

3.2 $L1_2$-Cu_3Pt, $L1_0$-CuPt, and $L1_2$-$CuPt_3$ Phases

The four-sublattice model was applied to describe the Gibbs free energies of the $L1_2$-Cu_3Pt, $L1_0$-CuPt, and $L1_2$-$CuPt_3$ phases in the present assessment. The Gibbs free energy equation for a four-sublattice phase using the compound energy formalism is:

$$\begin{aligned} G_m^{4sl} = & \sum_{i=\mathrm{Cu}}^{\mathrm{Pt}} \sum_{j=\mathrm{Cu}}^{\mathrm{Pt}} \sum_{k=\mathrm{Cu}}^{\mathrm{Pt}} \sum_{l=\mathrm{Cu}}^{\mathrm{Pt}} y_i^{(1)} y_j^{(2)} y_k^{(3)} y_l^{(4)} \, {}^0G_{i:j:k:l} \\ & + RT \frac{1}{4} \sum_{m=1}^{4} \sum_{i=\mathrm{Cu}}^{\mathrm{Pt}} y_i^{(m)} \ln y_i^{(m)} \\ & + y_{\mathrm{Cu}}^{(1)} y_{\mathrm{Pt}}^{(1)} \left(\sum_{k,l,m} y_k^{(2)} y_l^{(3)} y_m^{(4)} \, {}^0L_{\mathrm{Cu,Pt}:k:l:m} \right) + \ldots \\ & + y_{\mathrm{Cu}}^{(1)} y_{\mathrm{Pt}}^{(1)} y_{\mathrm{Cu}}^{(2)} y_{\mathrm{Pt}}^{(2)} \left(\sum_{p,q} y_p^{(3)} y_q^{(4)} \, {}^0L_{\mathrm{Cu,Pt:Cu,Pt}:p:q} \right) + \ldots \end{aligned} \qquad \text{(Eq 4)}$$

where $y_i^{(m)}$, ${}^0G_{i:j:k:l}$, and L are the site fraction of the element i on the sublattice m, compound energies, and interaction parameters, respectively. A colon in the suffix of compound energies and interaction parameters separates elements on different sublattices, and a comma separates elements on the same sublattice. The regular parameters, ${}^0L_{\mathrm{Cu,Pt}:k:l:m}$, in Eq 4, can be given approximately by the second nearest-neighbor interaction energy under the assumption of random mixing within each sublattice. It has been shown by the first-principles calculations[35] that the interaction energy of the second-neighbor pairs is far from negligible. The regular parameters are thus indispensable in the assessment. The fourth summation on the right-hand side is called the reciprocal term, which represents the contribution of the SRO to the Gibbs free energy.[47,48]

From the fact that the sublattices are identical and that the Gibbs free energy expression also represents the disordered state, the following relations must be fulfilled:

$$\begin{aligned} {}^0G_{\mathrm{Cu:Cu:Cu:Pt}} &= {}^0G_{\mathrm{Cu:Cu:Pt:Cu}} = {}^0G_{\mathrm{Cu:Pt:Cu:Cu}} = {}^0G_{\mathrm{Pt:Cu:Cu:Cu}} \\ &= 3^{(1)}v_{\mathrm{Cu:Pt}} + 3^0\alpha_{\mathrm{Cu_3Pt}} \\ {}^0G_{\mathrm{Cu:Cu:Pt:Pt}} &= {}^0G_{\mathrm{Cu:Pt:Cu:Pt}} = {}^0G_{\mathrm{Pt:Cu:Cu:Pt}} = {}^0G_{\mathrm{Cu:Pt:Pt:Cu}} \\ &= {}^0G_{\mathrm{Pt:Cu:Pt:Cu}} = {}^0G_{\mathrm{Pt:Pt:Cu:Cu}} = 4^{(1)}v_{\mathrm{Cu:Pt}} \\ {}^0G_{\mathrm{Cu:Pt:Pt:Pt}} &= {}^0G_{\mathrm{Pt:Cu:Pt:Pt}} = {}^0G_{\mathrm{Pt:Pt:Cu:Pt}} = {}^0G_{\mathrm{Pt:Pt:Pt:Cu}} \\ &= 3^{(1)}v_{\mathrm{Cu:Pt}} + 3^0\alpha_{\mathrm{CuPt_3}} \\ {}^0L_{\mathrm{Cu,Pt:*:*:*}} &= {}^0L_{\mathrm{*:Cu,Pt:*:*}} = {}^0L_{\mathrm{*:*:Cu,Pt,*}} = {}^0L_{\mathrm{*:*:*:Cu,Pt}} \\ {}^0L_{\mathrm{Cu,Pt:Cu:Cu:Cu}} &= {}^0L_{\mathrm{Cu,Pt:Pt:Pt:Pt}} = 1.5^{(2)}v_{\mathrm{Cu:Pt}} \\ {}^0L_{\mathrm{Cu,Pt:Cu:,Cu:Pt}} &= {}^0L_{\mathrm{Cu,Pt:Cu:Pt:Pt}} = 1.5^{(2)}v_{\mathrm{Cu:Pt}} + 1.5^0\beta \\ {}^0L_{\mathrm{Cu,Pt:Cu,Pt:*:*}} &= {}^0L_{\mathrm{Cu,Pt:*:Cu,Pt:*}} = {}^0L_{\mathrm{*:Cu,Pt:Cu,Pt:*}} = {}^0L_{\mathrm{Cu,Pt:*:*:Cu,Pt}} \\ &= {}^0L_{\mathrm{*:Cu,Pt:*:Cu,Pt}} = {}^0L_{\mathrm{*:*:Cu,Pt:Cu,Pt}} \cong {}^{(1)}v_{\mathrm{Cu:Pt}} + {}^0\gamma \end{aligned} \qquad \text{(Eq 5)}$$

where α, β, and γ are adjustable parameters, and ${}^{(n)}v_{\mathrm{Cu:Pt}}$ is the interaction energy of the n-th nearest-neighbor pairs. Those parameters were fitted to experimental data. The factors 3, 4, and 1.5 in front of the interaction energies originate from the number of bonds between Cu and Pt atoms in each ordered structure.

To simplify the integration of an ordered-fcc phase with a database where many systems have the A1 phase without any ordering, it is advantageous to partition the Gibbs free energy for an ordered phase into two parts:

$$G_m^{\mathrm{ord}} = G_m^{\mathrm{dis}}(x_i) + \Delta G_m^{\mathrm{ord}}(y_i) \qquad \text{(Eq 6)}$$

where $\Delta G_m^{\mathrm{ord}}(y_i) = 0$ when the phase is disordered; thus $G_m^{\mathrm{dis}}(x_i)$ contains all parameters needed to describe the disordered phase and is given by Eq 1. $\Delta G_m^{\mathrm{ord}}(y_i)$ is calculated using the sublattices, and one way to ensure that $\Delta G_m^{\mathrm{ord}}(y_i)$ is zero when the phase is disordered is by calculating Eq 4 twice: once with the original site fractions and once with them replaced by the mole fractions as:

$$\Delta G_m^{\mathrm{ord}} = G_m^{4\mathrm{sl}}(y_i) - G_m^{4\mathrm{sl}}(y_i = x_i) \qquad \text{(Eq 7)}$$

Another advantage of Eq 6 for describing the ordering of the A1 phase is that one may assess the parameters of $\Delta G_m^{\text{ord}}(y_i)$ without changing the description of the A1 phase.

It is possible to derive relations between the parameters of the ordered model Eq 4 and the excess parameter in Eq 3 from $G_m^{\text{dis}} = G_m^{4\text{sl}}(y_i = x_i)$. Relations between those parameters can be simply derived as shown in the following matrix:

$$\begin{pmatrix} {}^0L_{\text{Cu,Pt}} \\ {}^1L_{\text{Cu,Pt}} \\ {}^2L_{\text{Cu,Pt}} \\ {}^3L_{\text{Cu,Pt}} \end{pmatrix} = \begin{pmatrix} 1 & 3/2 & 1 & 1/2 & 3/2 & 3/2 & 1/2 & 3/2 & L0 \\ 2 & 0 & -2 & 3/2 & 3/2 & -3/2 & -3/2 & 0 & L1 \\ 1 & -3/2 & 1 & 3/2 & -3/2 & -3/2 & 3/2 & -3/2 & L2 \\ 0 & 0 & 0 & 1/2 & -3/2 & 3/2 & -1/2 & 0 & L3 \end{pmatrix} \begin{pmatrix} {}^0G_{\text{Cu:Cu:Cu:Pt}} \\ {}^0G_{\text{Cu:Cu:Pt:Pt}} \\ {}^0G_{\text{Cu:Pt:Pt:Pt}} \\ {}^0L_{\text{Cu,Pt:Cu:Cu:Cu}} \\ {}^0L_{\text{Cu,Pt:Cu:Cu:Pt}} \\ {}^0L_{\text{Cu,Pt:Cu:Pt:Pt}} \\ {}^0L_{\text{Cu,Pt:Pt:Pt:Pt}} \\ {}^0L_{\text{Cu,Pt:Cu,Pt:*:*}} \\ 1 \end{pmatrix} \quad \text{(Eq 8)}$$

where $L0$, $L1$, $L2$, and $L3$ are adjustable parameters and are fitted to experimental data.

3.3 $L1_1$-CuPt Phase

Although it is possible to introduce more sublattices to model the $L1_1$ phase together with the $L1_2$ and $L1_0$ phases, at least 8 sublattices are required. Eight or more sublattices might allow other superstructures in the Pt-rich region to be modeled together with the $L1_2$ and $L1_0$ phases to give a more physically appropriate treatment of those phases in the system. However, in view of further expansions to higher-order systems, it is obviously very difficult to handle, and the complexity due to the large number of sublattices in a model may become a great disadvantage. Thus, in the present assessment, the Gibbs free energy of the $L1_1$ phase was modeled separately from the $L1_2$ and $L1_0$ phases and was described by the two-sublattice model. The Gibbs free energy expression for the $L1_1$ phase with two sublattices can be given by:

$$G_m^{L1_1} = \sum_{i=\text{Cu}}^{\text{Pt}} \sum_{j=\text{Cu}}^{\text{Pt}} y_i^{(1)} y_j^{(2)}\, {}^0G_{i:j} + RT\frac{1}{2}\sum_{m=1}^{2}\sum_{i=\text{Cu}}^{\text{Pt}} y_i^{(m)} \ln y_i^{(m)}$$
$$+ y_{\text{Cu}}^{(1)} y_{\text{Pt}}^{(1)} \left(\sum_{k=\text{Cu}}^{\text{Pt}} y_k^{(2)} [{}^0L_{\text{Cu,Pt:}k} + {}^1L_{\text{Cu,Pt:}k}(y_{\text{Cu}}^{(2)} - y_{Pt}^{(2)})] \right)$$
$$+ y_{\text{Cu}}^{(2)} y_{\text{Pt}}^{(2)} \left(\sum_{k=\text{Cu}}^{\text{Pt}} y_k^{(1)} [{}^0L_{k\text{:Cu,Pt}} + {}^1L_{k\text{:Cu,Pt}}(y_{\text{Cu}}^{(1)} - y_{Pt}^{(1)})] \right)$$
$$+ y_{\text{Cu}}^{(1)} y_{\text{Pt}}^{(1)} y_{\text{Cu}}^{(2)} y_{\text{Pt}}^{(2)}\, {}^0L_{\text{Cu,Pt:Cu,Pt}} \quad \text{(Eq 9)}$$

where $y_i^{(m)}$, ${}^0G_{i:j}$, and L are the site fraction of element i on the sublattice m, the compound energies, and the interaction parameters, respectively.

Because both $L1_1$ and $L1_2$ phases are equivalent to the A1 phase in the disordered state, one can obtain Eq 10 from the relationships $G_m^{\text{dis}}(x_i) = G_m^{L1_1}(y_i = x_i) = G_m^{4\text{sl}}(y_i = x_i)$:

$$G_{\text{Cu:Pt}}^{L1_1} = G_{\text{Pt:Cu}}^{L1_1} = 3^{(1)}v_{\text{Cu:Pt}} + 3^{(2)}v_{\text{Cu:Pt}} + {}^0\alpha_{L1_1}$$
$${}^0L_{\text{Cu:Cu,Pt}} = {}^0L_{\text{Cu,Pt:Cu}} = 3^{(1)}v_{\text{Cu:Pt}} + {}^0\beta_{L1_1}$$
$${}^0L_{\text{Pt:Cu,Pt}} = {}^0L_{\text{Cu,Pt:Pt}} = 3^{(1)}v_{\text{Cu:Pt}} + {}^0\beta_{L1_1}$$
$${}^1L_{*\text{:Cu,Pt}} = {}^1L_{\text{Cu,Pt:}*} = {}^1\beta_{L1_1}$$
$${}^0L_{\text{Cu,Pt:Cu,Pt}} = 6L_{\text{Cu,Pt:Cu,Pt:*:*}} + {}^0\gamma_{L1_1} \quad \text{(Eq 10)}$$

where α, γ, and β are adjustable parameters and were fitted to experimental data.

4. Results

4.1 Comparison with Experimental Data

The selected set of parameters was optimized with the experimental data using the Parrot module[49] in the Thermo-Calc software package.[50] The calculated phase diagram is shown in Fig. 1. All parameters evaluated in the present work are listed in Table 1.

Figure 2(a) shows the calculated liquidus and solidus lines with experimental data plots. The calculated phase boundaries are in agreement with the experimental data. For smooth interpolation of liquidus and solidus lines in the Pt-rich region, where there is no experimental data, the assessment has been carried out under the assumption that the gradients of the liquidus and the solidus, with respect to the mole fraction of Pt, were kept positive all through the composition range.

A comparison of the calculated phase boundaries for solid phases with experimental data is shown in Fig. 2(b). The congruent points of $L1_2$-Cu_3Pt and $L1_1$-CuPt phases and their phase boundaries agree with experimental data, except for slight deviations found in $L1_1$/A1 phase boundaries in the Pt-rich region, where calculated phase boundaries are slightly shifted to lower temperatures than experimental data. The reason for the deviation is that the stable intermetallic phases in the Pt-rich region were not taken into consideration in the present assessment. In the present assessment, the resultant parameter set gives a rather wider A1 + $L1_2$ region in the Pt-rich side than was expected from the experimental data.[8,9] For an improvement in accuracy, ad-

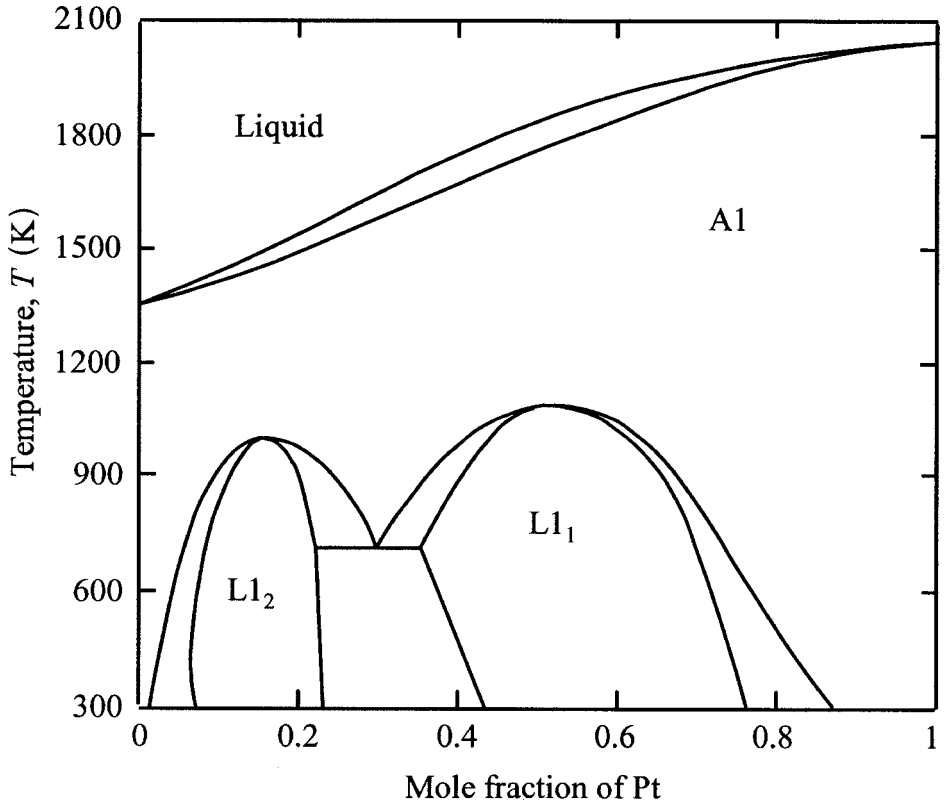

Fig. 1 Assessed Cu-Pt phase diagram

Table 1 Thermodynamic parameters for the Cu-Pt binary system (J/mol)

Parameter	
Liquid phase	**L1$_2$ phase**
${}^0L^{Liq}_{Cu,Pt} = -24{,}900 - 3.3T$	${}^{(1)}\nu_{Cu:Pt} = -18{,}090 + 6.9T$
${}^1L^{Liq}_{Cu,Pt} = -34{,}400 + 9.1T$	${}^{(2)}\nu_{Cu:Pt} = -20{,}400 + 7.53T$
${}^2L^{Liq}_{Cu,Pt} = +14{,}500 - 12.1T$	${}^0\alpha_{Cu3Pt} = -2270$
	${}^0\alpha_{CuPt3} = -1620$
FCC_A1 phase	${}^0\beta = +12{,}740$
$L0 = +250{,}900 - 107.8T$	${}^0\gamma = +17{,}300 - 16T$
$L1 = -5{,}200 - 1.24T$	
$L2 = +75{,}070 - 22.3T$	**L1$_1$ phase**
${}^0T_c^{mag}{}_{Cu,Pt} = 0$	${}^0\alpha_{L11} = +61{,}210 - 42.23T$
${}^0\beta^{mag}{}_{Cu,Pt} = 0$	${}^0\beta^{Cu}{}_{L11} = -48{,}150 - 20.9T$
	${}^0\beta^{Pt}{}_{L11} = -41{,}470 - 20.6T$
	${}^1\beta_{L11} = -1490 - 0.95T$
	${}^0\gamma_{L11} = -20{,}700 + 71.2T$

Note: Parameters for pure elements are taken from the compilation of Dinsdale.[45] T_c^{mag} and β^{mag} are the Curie temperature and the magnetic moment in Bohr magneton, respectively.

ditional experimental data on phase equilibria related to the A1, L1$_2$, L1$_1$ and LPS phases will be needed.

Figure 3 shows a metastable phase diagram at low temperature. In the present assessment, the L1$_2$-CuPt$_3$/A1 metastable phase boundary was kept at lower temperatures than the stable phase boundaries,[6] drawn with dotted lines in the figure. At 1:1 stoichiometry, the L1$_0$-CuPt phase is less stable than the A1 phase ($\Delta_f H = -11$ kJ/mol at 1:1 composition), as was predicted by first-principles calculations[35] and does not appear in the metastable phase diagram.

The calculated enthalpy of mixing in the A1 phase is in agreement with experimental data, as shown in Fig. 4. The activity of Cu has been measured over a wide range of temperatures. The assessed parameters can reproduce the activity data very well, as shown in Fig. 5. The calculated long-range order parameters of the L1$_1$-CuPt phase are in agreement with the experimental data, as shown in Fig. 6.

The formation enthalpies of the four stable/metastable ordered structures are listed in Table 2. The enthalpies of formation assessed in the current study, where Cu(A1) and Pt(A1) at 0 K were chosen as the reference states, are in agreement with those experimentally determined and estimated from the first-principles calculations.

The first and the second nearest-neighbor pair interactions obtained in the present assessment are also listed in Table 2. The ground state analysis, based on the first and the second nearest-neighbor pair interaction energies,[51-54] suggests that the variety of ordered structures will appear as stable phases depending on the sign and the ratio of those interaction energies. According to Büth et al.,[52] for the first and the second interaction energies obtained in the present assessment where ${}^{(1)}\nu_{Cu:Pt}$ is negative, and ${}^{(2)}\nu_{Cu:Pt}/{}^{(1)}\nu_{Cu:Pt}$ is positive and larger than 1/3, ordered structures $D0_{22}$ and L1$_1$ become stable at the ground state instead of the L1$_2$ and

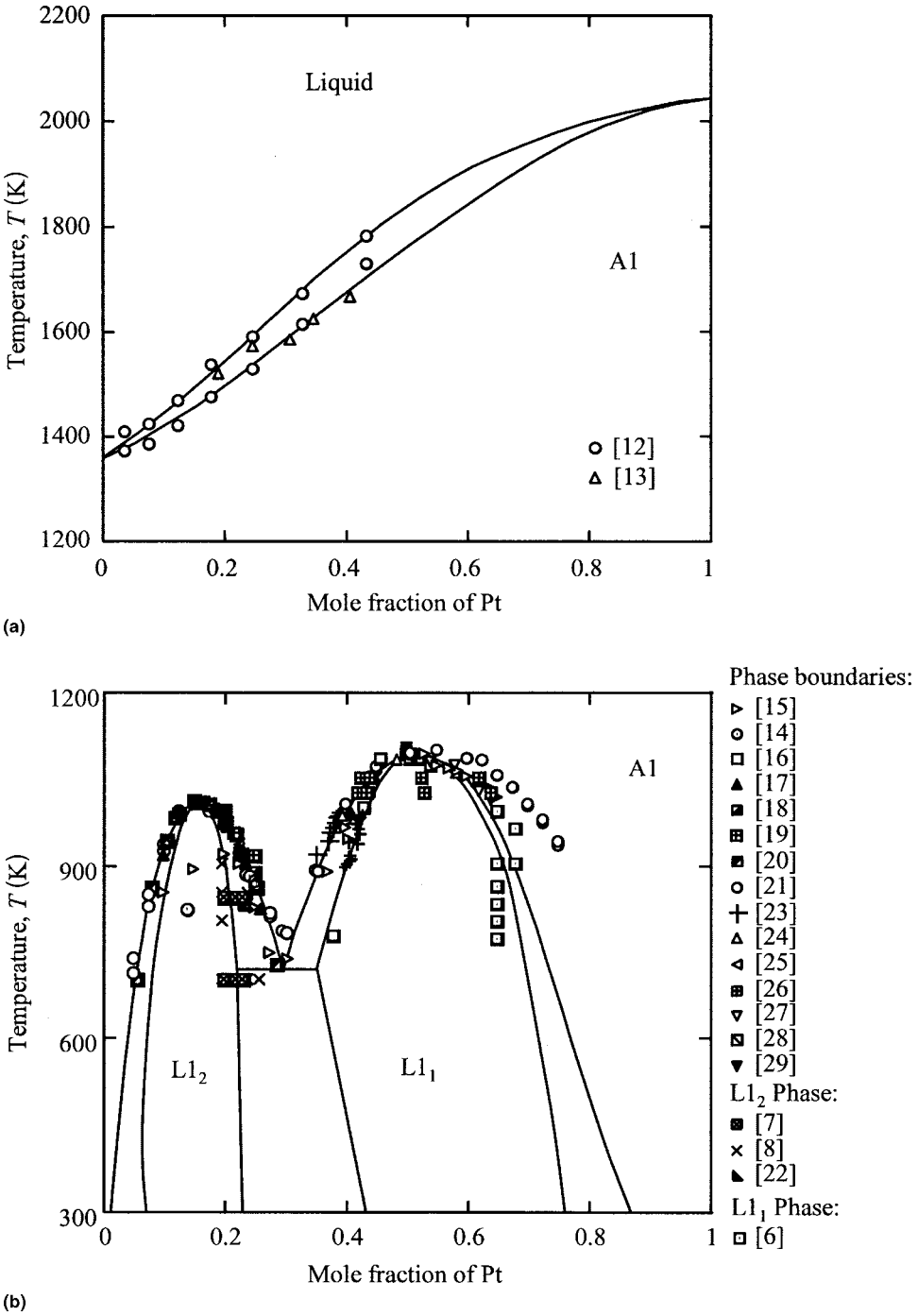

Fig. 2 Comparison of (a) calculated liquidus-solidus lines; (b) calculated ordering transformations with experimental data

$L1_0$ phases. However, as random mixing within a sublattice is assumed in the present model, ordering within each sublattice cannot occur. Thus, those ordered structures predicted by Büth et al.[52] degenerate to either $L1_2$ or $L1_0$ phases in the present sublattice setting.

4.2 Short-Range Order Parameter

For the A1 phase, the effects of SRO on the order-disorder transitions are much larger than those for the bcc(A2) phase,[48] and thus the effect should be taken into the Gibbs free energy to accurately model the order-disorder transitions in the Cu-Pt system. According to Abe et al.,[48] the short range order parameter in the nearest-neighbor shell, ε, for the A1 phase with the four sublattices is defined as:

$$p_{i:i}^{(k,l)} = y_i^{(k)} y_i^{(l)} - \varepsilon$$
$$p_{i:j}^{(k,l)} = y_i^{(k)} y_j^{(l)} + \varepsilon \quad \text{(Eq 11)}$$

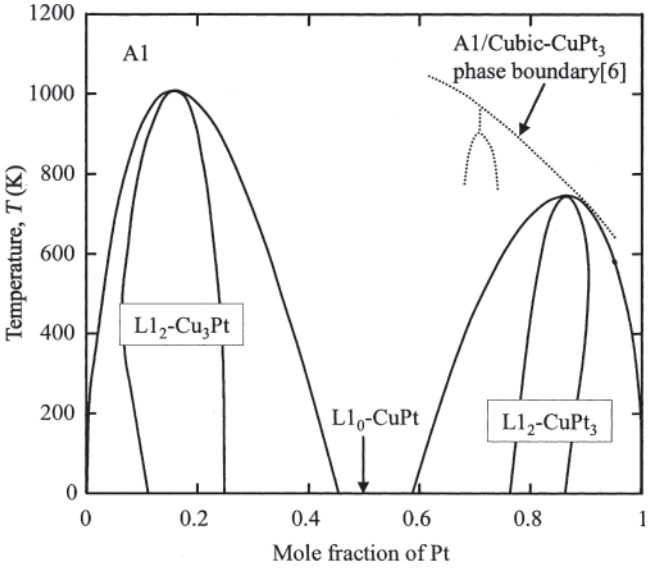

Fig. 3 Calculated $L1_2$/A1 phase boundaries. The peak temperature of the $L1_2$-$CuPt_3$/A1 phase boundary (solid line) is lower than the Cubic-$CuPt_3$/A1 phase boundary (dotted line).

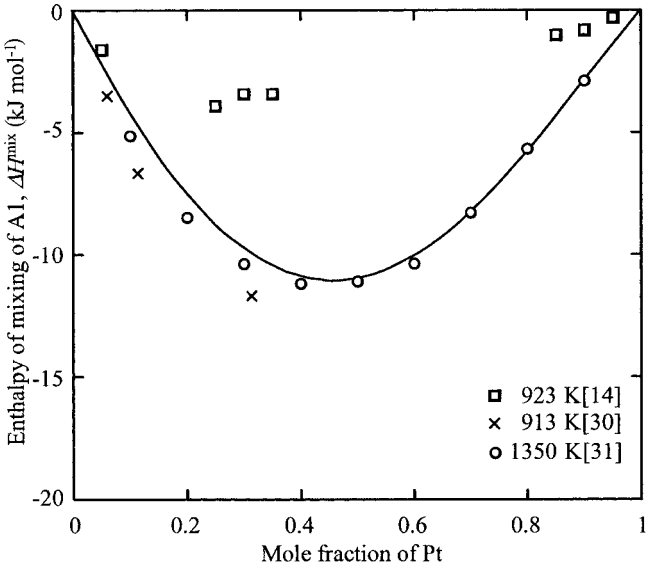

Fig. 4 Comparison of the calculated enthalpy of mixing in the A1 phase with experimental data

where $p_{i:j}^{(k,l)}$ is an *i-j* pair probability. The short range order parameter and the contribution of SRO to the Gibbs free energy are derived from a comparison between the Gibbs free energy functions based on the pair quasi-chemical model and the four-sublattice model. The Warren-Cowley short-range order parameter, ε_{WC}, is given by $\varepsilon_{WC} = -\varepsilon/x_i x_j$. Using the reciprocal parameters, it then becomes:

$$\varepsilon_{WC} = \frac{2x_{Cu}x_{Pt}{}^{(1)}v_{Cu:Pt}}{RT} = -x_{Cu}x_{Pt}\left(\frac{-2^0L_{Cu,Pt:Cu,Pt:*:*}}{RT}\right)^{0.5} \quad \text{(Eq 12)}$$

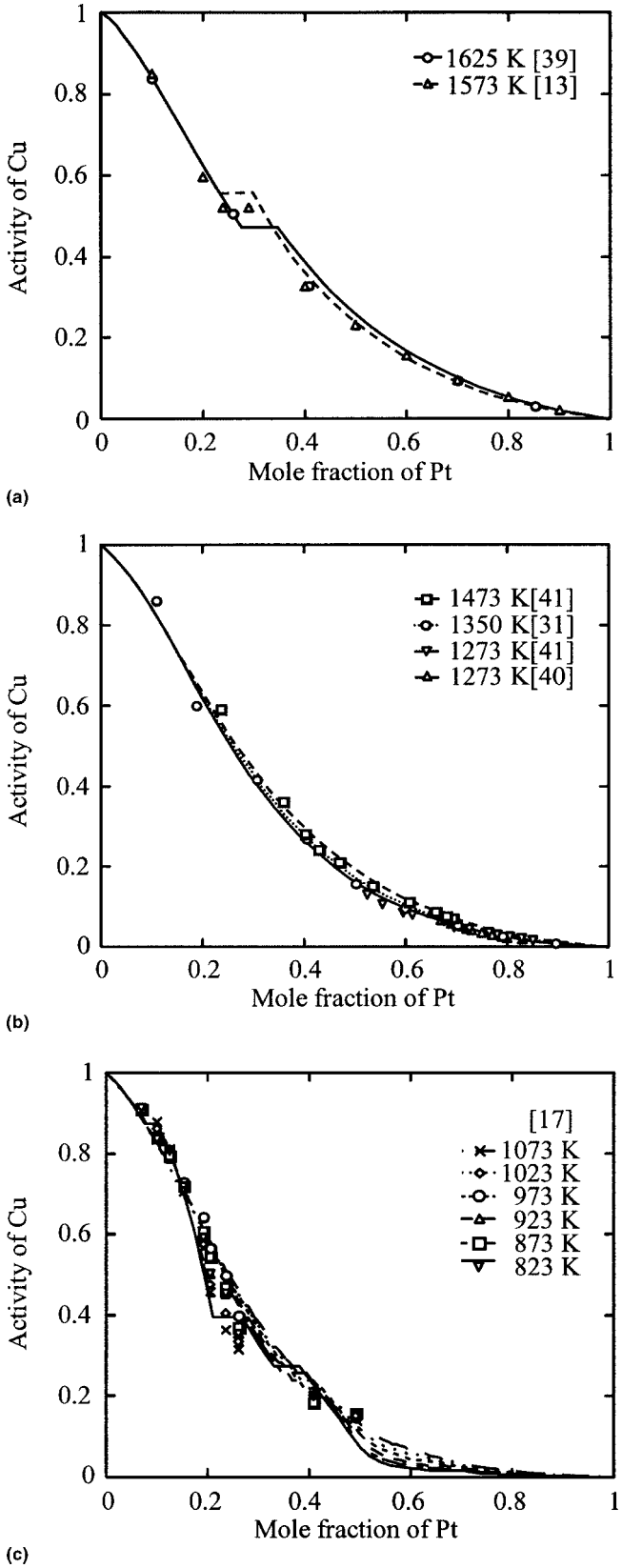

Fig. 5 Calculated activity of Cu (a) at 1573 and 1625 K; (b) at 1273, 1350, and 1473 K; and (c) at 823-1073 K with experimental data

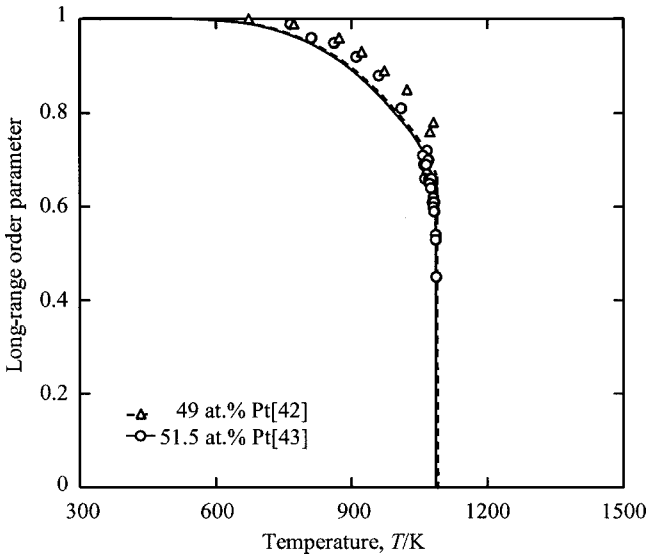

Fig. 6 Calculated long-range order parameter for the $L1_1$ phase with experimental data as a function of temperature

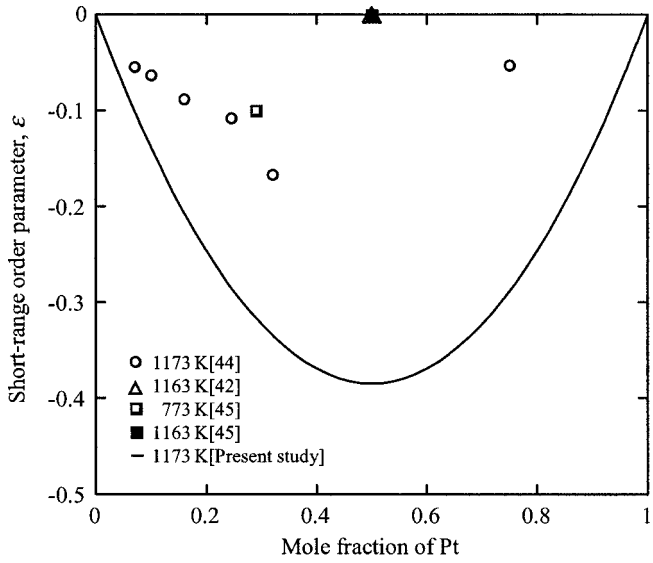

Fig. 7 Estimated Warren-Cowley short-range order parameter for the A1 phase with experimentally determined short range order parameters for the first nearest-neighbor shell

Table 2 Enthalpies of formation and interaction energies between the *n*th nearest neighbor atoms, $^{(n)}\nu_{Cu:Pt}$, in the Cu-50 at.% Pt alloy (kJ/mol)

Enthalpy of formation, $\Delta_f H$				Interaction energy			
$L1_2$-Cu_3Pt	$L1_0$-CuPt	$L1_1$-CuPt	$L1_2$-$CuPt_3$	$^{(1)}\nu_{Cu:Pt}$	$^{(2)}\nu_{Cu:Pt}$	Method	Reference
−14	−13	…	−14	…	…	LMTO	[37]
−11.2	−9.5	−12.4	−9.3	−17	−5	LAPW	[35]
−11	−11	−20	−13	−20	−5	ASW	[34, 36]
−13	…	−18	−10	…	…	Miedema	[38]
−10.8	…	…	…	…	…	Exp.	[33]
…	…	−15.6	…	…	Exp.	Exp.	[30]
−11.0	−9.6	−16.0	−8.0	−18	−8	…	Present study

LMTO, linear muffin-tin orbital method; LAPW, linearized augmented plane wave method; ASW, augmented spherical wave method.

The contribution of SRO to the Gibbs free energy of the A1 phase, ΔG_m^{SRO}, is given by:

$$\Delta G_m^{SRO} = 6x_{Cu}^2 x_{Pt}^2 {}^0L_{Cu,Pt:Cu,Pt:*:*} \quad \text{(Eq 13)}$$

Using the interaction parameters in the four sublattice model, the Redlich-Kister coefficients of the A1 phase are given as shown in Eq 8, where the contribution of short range order to the Gibbs free energy of the A1 phase, given by Eq 13, is taken through the reciprocal parameters in the excess Gibbs free energy term in the substitutional solution model.

Figure 7 shows a comparison between the short range order parameter from Eq 12 and the measured short range order parameter in the first nearest-neighbor shell. According to Walker,[42] at the equiatomic composition, the short range order parameter in the nearest-neighbor shell is almost 0. He attributed this result to the local structure just above the critical temperature, when the atoms on average manage to maintain local layering configurations, partially segregating onto alternate (111) planes. If the local structure of the disordered phase would inherit ordered structures, the behavior of the short range order would not be simple, because various kinds of ordered structures were observed in this system.

Compared with experimental data, the calculated short range order parameter is a larger negative in all composition ranges, particularly near the equiatomic composition. Although Eq 12 is derived from the pair approximation, the short range order parameter includes not only the contribution of the short range order in the nearest-neighbor shell but also those of the higher-order shells. This is one of the reasons why Eq 12 gives larger negative values compared with experimental data.

For the case where the accurate description of short range order is required, one may have to introduce more sublattices or should consider other thermodynamic models, such as CVM.

5. Conclusions

Thermodynamic assessment of the Cu-Pt system was performed using the sublattice models where the SRO is explicitly taken into account through reciprocal parameters. A consistent set of parameters for the phases in the Cu-Pt system was obtained. The calculated stable and metastable phase boundaries are in agreement with experimental data. The calculated enthalpy of mixing in the A1 phase, the enthalpy of formation for ordered phases, activities of Cu, and the long-range order parameter in the $L1_1$-CuPt are in agreement with experimental data.

Acknowledgments

The authors thank Dr. Takizawa of Hokkaido University for discussions and comments on the first-principles calculations. The present research is partly supported by a Grant-in-Aid for Scientific Research (No. 428-15074220) from the Japan Society for the Promotion of Science. The support from Core Research for Evolutional Science and Technology (CREST), Japan Science and Technology Agency, is acknowledged.

References

1. B.D. Chandler, A.B. Schabel, and L.H. Pignolet, Preparation and Characterization of Supported Bimetallic Pt-Au and Pt-Cu Catalysts from Bimetallic Molecular Precursors, *J. Catal.,* 2000, 193, p 186-198
2. F. Epron, F. Gauthard, and J. Barbier, Influence of Oxidizing and Reducing Treatments on the Metal-Metal Interactions and on the Activity for Nitrate Reduction of a Pt-Cu Bimetallic Catalyst, *Appl. Catal. A,* 2002, 237, p 253-261
3. T. Maeda, A. Kikitsu, T. Kai, T. Nagase, H. Aikawa, and J. Akiyama, Effect of Added Cu on Disorder-Order Transformation of $L1_0$-Fe-Pt, *IEEE Trans. Magn.,* 2002, 38, p 2796-2798
4. Y.K. Takahashi, M. Ohnuma, and K. Hono, Effect of Cu on the Structure and Magnetic Properties of FePt Sputtered Film, *J. Magn. Mag. Mater.,* 2002, 246, 259-265
5. P.R. Subramanian and D.E. Laughlin, *Phase Diagrams of Binary Copper Alloys,* ASM International, 1993, 326-337.
6. R. Miida and D. Watanabe, Electron Microscope and Diffraction Study on the Ordered Structures of Platinum-Rich Copper-Platinum Alloys, *J. Appl. Crystallogr.,* 1974, 7, p 50-59
7. K. Schubert, B. Kiefer, M. Wilkens, and R. Haufler, On Some Metallic Ordered Phases with Long Periods, *Z. Metallkd.,* 1955, 46, p 692-715
8. S. Ogawa, H. Iwasaki, and A. Terada, Study of the Long-Period Ordered Alloy Cu_3Pt, *J. Phys. Soc. Jpn.,* 1973, 34, p 384-390
9. I.E. Dobrovinskii, V.V. Mechev, S.M. Vinikovskii, and V.A. Linkov, Activity of the Components in the Copper-Platinum System, *Izv. VUZ Tsvetn. Metall.,* 1973, 16, p 25-28, in Russian
10. V. Gopichand, S.S. Balakrishna, and A.K. Mallik, Systematics of Copper Base Binary Phase Diagrams, *CALPHAD,* 1980, 4, p 109-122
11. J.R. Taylor, Thermodynamic Assessment of Platinum Group Metal Systems-The Optimization of Binary Phase Diagrams, *Platinum Met. Rev.,* 1985, 29, p 74-80
12. F. Doerinckel, On Some Platinum Alloys, *Z. Anorg. Chem.,* 1907, 54, p 333-356, in German
13. Y.G. Park and D.R. Gaskell, The Thermodynamic Activities of Copper and Iron in the System Copper-Iron-Platinum at 1300°C, *Metall. Trans. B,* 1989, 20B, p 127-135
14. F. Weibke and H. Matthes, Electromotive Force in the System Platinum-Copper and Their Thermodynamic Evaluation, *Z. Electrochem.,* 1941, 47, p 421-432
15. A. Schneidner and U. Esch, The System Copper-Platinum, *Z. Electrochem.,* 1944, 50, p 290-301
16. A.A. Rudnitskii, Thermoelectric Method of Studying Transformations in Metals and Alloys, *Zh. Neorg. Khim.,* 1956, 6, p 1305-1321, in Russian
17. L.R. Bidwell, W.J. Schulz, and R.K. Saxer, The Activity of Solid Copper-Platinum Alloys and Some Observations on the Ordering of Cu_3Pt, *Acta Metall.,* 1967, 15, p 1143-1151
18. E.W. Collings, R.D. Smith, and J.C. Ho, Magnetic Investigations of Order-Disorder Transformations in Copper-Platinum (12.5-27.5 at.%) Alloys, *J. Less-Common Met.,* 1976, 46, p 189-195
19. E.V. Kozlov, A.S. Tailashev, Y.A. Savanov, and A.A. Klopotov, Study of the Ordered State of a Copper-Platinum (Cu_3Pt) Alloy with Periodic Antiphase Boundaries, *Strukt. Mekh. Faz. Prev. Met. Splavov,* 1976, p 146-149, in Russian
20. K. Mitsui, Y. Mishima, and T. Suzuki, Heterogeneous Ordering and Antiphase Domain Morphology in Cu_3Pt (19 at.% Pt), *Phil. Mag. A,* 1986, 53, p 357-376
21. K. Mitsui and M. Takahashi, Effect of Ternary Addition on the Formation of Cu_3Pt and CuPt Order Phases in the Cu-Pt System, *Phil. Mag. Lett.,* 1998, 77, p 49-57
22. M. Yodogawa, D.-M. Wee, Y. Oya, and T. Suzuki, The Morphology of Antiphase Domains of Cu_3Pt and Cu_3Au-Ni Alloys, *Scr. Metall.,* 1980, 14, p 849-854
23. N. Kuwano, T. Urazono, and K. Oki, Decomposition Process from $L1_1$ to ($A1+L1_1$) Involving First-Order Transformation in a Cu-Pt Alloy, *Mater. Trans. JIM,* 1991, 32, p 438-444
24. N.S. Kurnakov and V.A. Nemilow, On the Alloys of Platinum with Copper, *Z. Anorg. Chem.,* 1933, 210, p 1-12, in German
25. P. Assayag and M. Dode, Experimental Thermodynamic Study of the Superlattice of CuPt, *Compt. Rend. Acad. Sci.,* 1954, 239, p 762-764, in French
26. P. Assayag, Contribution to the Study of the Thermodynamic Properties of Copper-Platinum Alloys, *Ann. Chem.,* 1955, 10, p 637-665, in French
27. R.S. Irani and R.W. Cahn, A Classical Phase Transformation: Order-Disorder in CuPt, *Nature,* 1970, 226, p 1045-1046
28. K. Hisatsune, M. Ohta, and M. Yamane, Coexistent Region of Ordered and Disordered Phases in CuPt, *Scr. Metall.,* 1977, 11, p 563-564
29. G.W. Geiken, "A Thermodynamic Study of the Heat of Ordering in CuPt," USAEC Report UCRL-17615, University of California-Berkeley, 1967
30. R. Oriani and W.K. Murphy, Thermodynamics of Ordering Alloys-IV. Heats of Formation of Some Alloys of Transition Metals, *Acta Metall.,* 1962, 10, p 879-885
31. K.L. Myles and J.B. Darby, Jr., Thermodynamic Properties of Solid Palladium-Copper and Platinum-Copper Alloys, *Acta Metall.,* 1968, 16, p 485-492
32. R. Hultgren, P.D. Desai, D.T. Hawkins, M. Gleiser, K.K. Kelly, and D. Wagman, *Selected Values of the Thermodynamic Properties of the Elements,* Materials Park, Ohio, 1973, p 782-786
33. S.V. Meschel and O.J. Kleppa, Thermochemistry of Some Binary Alloys of Noble Metals (Cu, Ag, Au) and Transition Metals by High Temperature Direct Synthesis Calorimetry, *J. Alloys Compd.,* 2003, 350, p 205-212

34. S. Takizawa, K. Terakura, and T. Mohri, Electronic Theory for Phase Stability of Nine *AB* Binary Alloys, with *A* = Ni, Pd, or Pt and *B* = Cu, Ag, or Au., *Phys. Rev. B,* 1989, 39, p 5792-5797
35. Z.W. Lu, S.H. Wei, A. Zunger, S. Froto-Pessoa, and L.G. Ferriera, First-Principles Statistical Mechanics of Structural Stability of Intermetallic Compounds, *Phys. Rev. B,* 1991, 44, p 512-544
36. S. Takizawa, A New Phase of Cu-Pt Alloy-Theoretical Prediction and Experimental Support, *J. Phys. Soc. Jpn.,* 1996, 65, p 2178-2181
37. G.H. Johannesson, T. Bligaard, A.V. Ruban, H.L. Skriver, K.W. Jacobsen, and J.K. Nørskov, Combined Electronic Structure and Evolutionary Search Approach to Materials Design, *Phys. Rev. Lett.,* 2002, 88, p 255506-1-255506-5
38. FR. de Boer, R. Boom, W.C.M. Mattens, A.R. Miedema, and A.K. Niessen, Cohesion in Metals, *Transition Metal Alloys,* Elsevier Science, Amsterdam, The Netherlands, 1988, p 619-637
39. J.M. McCormack, J.R. Myers, and R.K. Saxer, Thermodynamic Properties of Copper-Platinum Alloys, *Trans. Metall. Soc. AIME,* 1966, 236, p 1635-1637
40. N.G. Schmahl and E. Minzl, Determination of Copper Activities in Cu-Pt and Cu-Au Alloys with the Aid of Oxygen Decomposition Pressures, *Z. Phys. Chem.,* 1965, 47, p 164-182
41. C. Landolt and A. Muan, Activity-Composition Relations in Solid Cu-Pt Alloys as Derived from Equilibrium Measurements in the System Cu-Pt-O at 1000°C and 1200°C, *Trans. Metall. Soc. AIME,* 1969, 245, p 791-796
42. C.B. Walker, X-Ray Measurement of Order in CuPt, *J. Appl. Phys.,* 1952, 23, p 118-123
43. H. Lang, T. Mohri, and W. Pfeiler, $L1_1$ Long-Range Order in CuPt: A Comparison Between X-Ray and Residual Resistivity Measurements, *Intermetallics,* 1999, 7, p 1373-1381
44. D.K. Saha and K. Ohshima, Short-Range Order in Cu-Pt Alloys, *J. Phys. Condens. Matter.,* 1993, 5, p 4099-4110
45. I.G. Batirev, A.A. Katsnelson, L. Kertész, and A. Szász, Coherent Potential Approximation of Short-Range Order in Cluster Model of Alloys, *Phys. Stat. Sol.,* 1980, 101, p 163-168
46. A.T. Dinsdale, SGTE Data for Pure Elements, *CALPHAD,* 1991, 15, p 317-425
47. B. Sundman, S.G. Fries, and W.A. Oates, Incorporation of Cluster Expansion Theory into the Compound Energy Formalism, *CALPHAD,* 1998, 22, p 335-357
48. T. Abe and B. Sundman, A Description of the Effect of Short Range Ordering in the Compound Energy Formalism, *CALPHAD,* 2003, 27, p 403-408
49. B. Jansson, "Evaluation of Parameters in Thermochemical models using Different Types of Experimental Data Simultaneously," Ph.D. dissertation, Royal Institute of Technology, Stockholm, Sweden, 1984
50. B. Jansson, M. Schalin, M. Selleby, and B. Sundman, The Thermo-Calc Database System, *Computer Software in Chemical and Extractive Metallurgy,* C.W. Bale and G.A. Irons, Eds., The Metals Society of CIM, Quebec, 1993, p 57-71
51. M.J. Richard and J.W. Cahn, Pairwise Interactions and the Ground State of Ordered Binary Alloys, *Acta Metall.,* 1971, 19, p 1263-1277
52. J. Büth and G. Inden, Ordering and Segregation Reactions in fcc Binary Alloys, *Acta Metall.,* 1982, 30, p 213-224
53. J. Kanamori and Y. Kakehashi, Conditions for the Existence of Ordered Structure in Binary Alloy Systems, *J. Phys., Paris,* 1977, 38, p C7-274-C7-279.
54. S.C. Moss and P.C. Clapp, Correlation Functions of Disordered Binary Alloys III, *Phys. Rev.,* 1968, 171, p 764-777